


Laser-induced thermocapillary convection in thin liquid layers: effect of thermal conductivity of substrates

A. Yu. Zykov¹ · N. A. Ivanova² 

Received: 18 April 2017 / Accepted: 12 August 2017 / Published online: 23 August 2017
© Springer-Verlag GmbH Germany 2017

Abstract The effect of the thermal conductivity of solid substrates on the thermocapillary convection induced by the thermal action of a laser beam in a thin liquid layer is studied experimentally. A diameter of photothermocapillary signal presenting a circular interference pattern formed on a screen by a probe laser beam reflected from the thermocapillary dimple is used for quantitative analysis. It is shown that diameter of the photothermocapillary signal changes with the thermal conductivity of substrates as k^{-n} . This suggests that the thermal conductivity of substrate strongly affects the curvature of thermocapillary dimple. An influence of the power of the heating laser beam and the liquid layer thickness on the sensitivity of the thermocapillary effect to the thermal conductivity of substrates is also studied. It was shown that the sensitivity of the photothermocapillary effect to the thermal conductivity of substrates increases with the power of the heating laser beam and decreases with increasing the thickness of the liquid layer.

1 Introduction

Thermocapillary convection induced by a thermal action of the laser irradiation in a thin liquid layer on a solid substrate [1–10] is of great importance in a wide range of applications, including the laser diagnostics of liquids [7–9, 11–17], nondestructive evaluation control of solids [18–20], and the

liquid-assisted laser cleaning of solid surfaces [21, 22]. An important feature of the laser-induced thermocapillary convection is that in the thin liquid layer in an area of stationary laser spot a concave deformation (called as a thermocapillary dimple) of the free liquid surface appears and the partially reflected from this deformation laser irradiation forms on a remote screen a circular interference pattern [7–10]. Da Costa and co-workers in their pioneering works [7–9] on investigation of the laser-induced thermocapillary deformation of the heavy oil layers noticed that thermal, mechanical and optical properties of liquids could be determined from the interference pattern [7–9]. Later, Bezuglyi and co-workers [6, 11–20] found out that the stationary diameter of the pattern (named subsequently as a photothermocapillary signal, PTC signal for short) depends on various parameters of an experimental arrangement (thickness of liquid layer and substrate, power and intensity distribution in a laser beam) and thermophysical properties of liquid and substrate. Basing on these findings a number of the non-contact photothermocapillary methods for measuring the thickness of transparent liquid layer on flat substrates [11, 12], viscosity of liquids [13], as well as a new method for measuring the contact angles of liquids on solid surfaces [14] have been developed. In [15, 16] a lag time between the switch-on moment of the laser beam and appearance of the PTC signal on a screen was detected. The deviation of the lag time from its quadratic change with the thickness of liquid layer was considered as a basis for development of a method for measuring the thermal diffusivity of liquids [15] and for monitoring of organic impurities on water surfaces [16]. Note that the liquids used in all mentioned experiments were optically transparent, and the thermal effect of the laser beam was achieved by absorption of the laser irradiation by solid substrates such as ebonite or carbolite.

✉ N. A. Ivanova
n.ivanova@utmn.ru

¹ Department of Physics, Industrial University of Tyumen, Volodarskogo 38, Tyumen 625000, Russia

² Photonics and Microfluidics Lab, Tyumen State University, Volodarskogo 6, Tyumen 625003, Russia

Several subsequent papers [18, 19] reported a new photo-thermocapillary approach to the non-destructive evaluation control of solid samples, based on analysis of the stationary PTC signal coming from the thermocapillary dimple of a transparent liquid layer on a solid substrate with different hidden flaws. A possibility to detect in solid samples of caverns and highly heat-conductive foreign inclusions under varnish and paint coatings was shown [18, 19].

Despite of comprehensive and longstanding studies of the laser-induced thermocapillary convection the influence of the thermal conductivity of solid substrates has been overlooked until now. This influence, however, may prove to be a very crucial because the laser irradiation is absorbed by a substrate resulting in a two-dimensional heat source at the interface between liquid and solid. The solid substrate definitely serves as a heat sink dissipating the energy from the heat source in accordance with its thermal conductivity. As it was shown in [23] temperature distribution on the free surface of liquid layer rested on a solid substrate depends on the thermal conductivity of this substrate. In turn the changing the surface temperature in our case leads to the changing geometrical parameters of the thermocapillary dimple and, consequently, the PTC signal. Thus, the thermal conductivity of substrate can affect not only sensitivity but also applicability of the proposed methods of the laser diagnostics of materials [6, 11–20]. Note that the thermal conductivity of substrates plays a key role in wide range of physical problems, including the spreading of liquids on solid substrates [24] where thermal resistance between liquid and solid influences the spreading rate and the flow pattern.

In this paper, we investigate the sensitivity of the laser-induced thermocapillary effect to the thermal conductivity of solid substrates using the stationary PTC signal. Moreover, we anticipate that results obtained may be taken as a basis for a new laser method for the thermal conductivity measurements of solid materials.

2 Formation of the thermocapillary dimple and the PTC signal

This section gives a brief description of the mechanism of the laser-induced thermocapillary convection and the PTC signal formation, see Fig. 1. When the heating laser beam, P_h , is incident on an absorbing solid substrate covered with a thin transparent liquid layer a heat source at the solid–liquid interface arises. The heat from this source distributes both into the depth of substrate and into the bulk of liquid layer. As a result, after a lag time [9, 15] written as

$$\tau_d = h_1^2 / 4\kappa_1 \quad (1)$$

the temperature of the free liquid surface increases that leads to a local decrease in the surface tension,

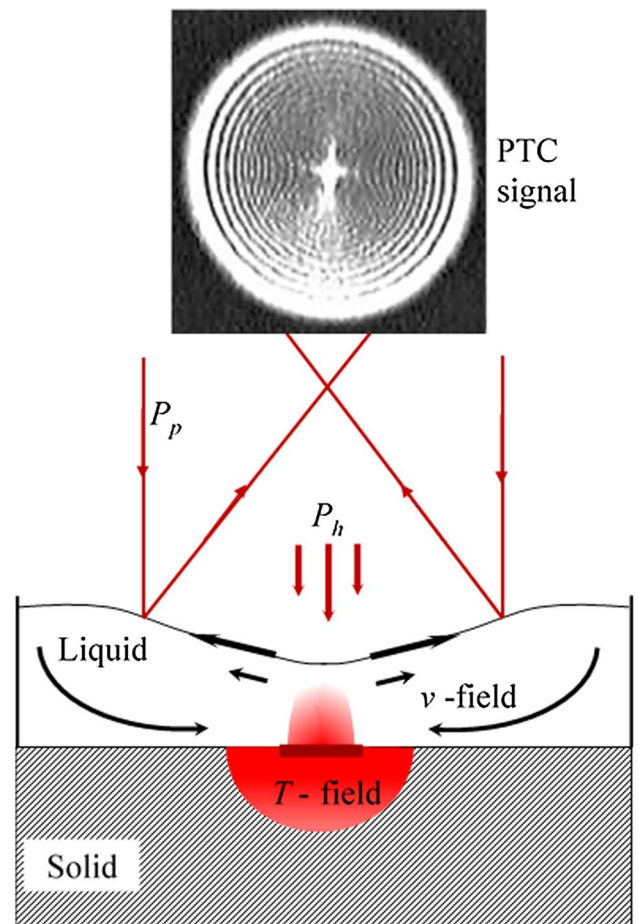


Fig. 1 Illustration of the thermocapillary deformation of a liquid layer caused by heating of a substrate with a laser beam and the formation of the photothermocapillary (PTC) signal by a probe laser beam. Temperature distribution (T -field) in both solid and liquid media as well as the velocity flows (v -field) in the liquid layer is depicted

$$\gamma = \gamma_0 + \gamma'_T(T - T_0), \quad (2)$$

where h_1 is the thickness of the liquid layer, κ_1 is the thermal diffusivity of the liquid; γ_0 is the surface tension of the liquid at a reference temperature T_0 ; $\frac{\partial \gamma}{\partial T} \equiv \gamma'_T$ is the thermocapillary coefficient, which is negative for most pure liquids. Consequently, a radially outward surface tension gradient along the free liquid surface arises:

$$\frac{\partial \gamma}{\partial r} = \frac{\partial \gamma}{\partial T} \frac{\partial T}{\partial r} > 0, \quad (3)$$

which is balanced by the velocity gradient in the bulk layer

$$\mu \frac{\partial v_r}{\partial z} = \frac{\partial \gamma}{\partial T} \frac{\partial T}{\partial r}, \quad (4)$$

where $\frac{\partial T}{\partial r}$ is the radial gradient of the surface temperature, v_r is the radial velocity of the liquid, z is the vertical

coordinate, and μ is the dynamic viscosity of the liquid. This process induces the radially outward thermocapillary flows, which lead to a lowering the liquid level and appearance of a thermocapillary concave deformation of the liquid layer in the irradiated spot. A negative capillary pressure below the curved surface causes the reverse bottom flow towards the heated spot, wherein it conjoins with the radially outward surface flows resulting in the thermocapillary toroidal convective vortex. Interestingly, that the deformed liquid interface represents a kind of optical element consisting of two mirrors separated by an inflection line: the one is a central concave mirror and the other is an annular convex mirror. A probe laser beam with the power $P_p \ll P_h$ reflected from this optical element forms a circular interference pattern on a remote screen, called as the PTC signal, Fig. 1. Note that in contrast to the classical Newton's fringes the PTC signal has the bright and wide outer ring, see Fig. 1. As it was found in [15, 16], the PTC signal goes through several stages: a signal delay lasting τ_d , then a fast increase of its diameter, which is related with the development of the thermocapillary convection and the dimple formation in the liquid layer and, finally, a slow increase of the PTC diameter up to reaching the stationary diameter, D_{st} . The latter indicates onset of the stationary thermocapillary dimple and the steady-state thermocapillary flows in the layer. The diameter of the PTC signal is directly related to the curvature of the thermocapillary dimple [6].

3 Experimental methods and materials

3.1 Substrates and fluidic cells preparation

The solid materials in a wide range of the thermal conductivity values from 0.13 to 117 W/(m K) were used as substrates. The thermophysical properties of those materials are listed in Table 1. The substrates in the form of disks of 60 mm in diameter and 20 mm in thickness were prepared as follows: using ebonite, PMMA and Teflon samples the disks were machined on a lathe. Metallic substrates such as Wood's metal, Rose's metal, Pb, Sn, and Zn were prepared by melting of granules of those materials in cylindrical duralumin dishes. After solidification, the working surfaces of those substrates were smoothed by polishing with a soft abrasive paper. The disks (~50 mm in diameter and 6 mm thick) of KRS-5 (thallium bromiodide crystal), BK7, quartz glass, KBr, NaCl, and CaF₂, placed in duralumin dishes were used as glass substrates. A marble slab of surface area of 100 mm² and 20 mm thickness was also used as a substrate. For convenience, in further experiments all substrates were conditionally divided into two types: the low heat-conductive (LHC) substrates with $k_s \leq 9.7$ W/(m K), and the highly heat-conductive (HHC) substrates with $k_s \geq 9.7$ W/(m K).

Table 1 Thermophysical properties of the substrate materials

Substrate materials	ρ_s , kg/m ³	C_p , J/(kg K)	K_s , W/(m K)	T , K	Refs.
Ebonite	916.2	1905	0.13	293	[30]
PMMA	1180	–	0.17	293	[29]
Teflon	2200	1050	0.25	293	[29]
TlBr-TlI (KRS-5)	7372	160	0.32	300	[26]
BK7	2510	858	1.11	300	[26]
Quartz glass	2210	730	1.4	293	[27]
Marble	2710	812	2.9	–	[28]
KBr	2749	440	4.8	300	[26]
NaCl	2164	869.9	6.5	300	[26]
CaF ₂	3181	911.3	9.7	300	[26]
Wood's metal	9730	147	12.8	293	[27]
Rose's metal	–	–	16	273	[25]
Lead (Pb)	11,340	127	35	293	[27]
	11,373	130	35	293	[29]
Tin (Sn) ^a	7290	221	62.8	293	[27]
	7304	228	67	293	[29]
Zinc (Zn) ^a	7130	385	113	296	[27]
	7144	388	121	293	[29]

^aAn average value of k_s was used to plot the graphs

The fluidic cells were constructed by attaching to all these substrates the stopper rings of PVC tape of 50–60 mm in diameter using an epoxy resin. To avoid an outflow of the working liquid, which may be caused by a capillary action, the height of the rings was around 10 mm. To ensure the same absorption of the heating laser beam by substrates with different optical properties, on their working surfaces the writing-ink (“Edding T25”, Germany) covering the area of 20 mm in diameter was deposited. After the ink was evaporated the dry coating film of around 10 μ m thickness, completely absorbed the laser radiation was formed. Below, this coating film is called as the heated area.

3.2 Experimental setup and method

The experimental setup is shown in Fig. 2. The beam of He–Ne laser ($P_h = 21$ mW maximum value, wavelength $\lambda = 633$ nm, beam diameter $d = 2.5$ mm) serving as the heating beam for generation of thermocapillary convection is directed normally to the substrate and absorbed by the heated area. The power of the heating beam was varied depending on experimental requirements using a calibrated optical wedge. The probe laser beam (He–Ne laser, $P_p = 0.3$ mW, $\lambda = 633$ nm, $d > 5$ mm) defocused with a spherical mirror is directed to the thermocapillary dimple. The probe beam being reflected from the free liquid surface forms the PTC signal on a screen. The experimental procedure was as follows. Silicon oil ($\mu = 4.6$ mPa s,

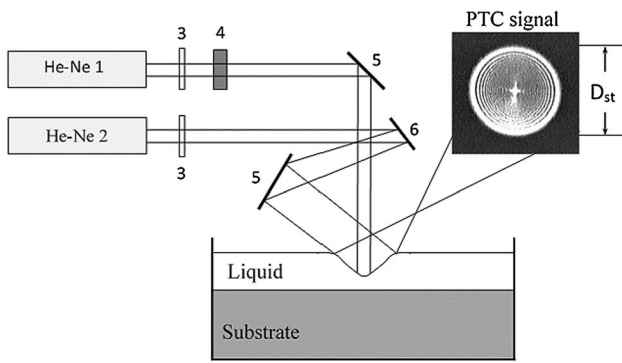


Fig. 2 Schematic view of the experimental setup. 1 The heating He-Ne laser (max power 21 mW), 2 the probe He-Ne laser (max power 0.3 mW), 3 shutters, 4 calibrated optical wedge, 5 mirrors, 6 spherical mirror

$\gamma = 19.7$ mN/m, $\gamma'_T \cong 0.06$ mN/m K, $k_1 = 0.12$ W/m K, $C_p = 1.5$ kJ/(kg K), $\rho = 920$ kg/m³, $\beta = 1.05 \times 10^{-3}$ 1/K [31]) was used as working liquid. A thin layer of silicon oil was deposited in a fluidic cell and its thickness was controlled using the method of the calibrated wires [12–15]. To exclude the influence thermo-gravitational convection in the process of the thermocapillary deformation, the thicknesses of layers were chosen to be below a critical thickness $h_1 < h_c = \left(\frac{\gamma'_T}{\rho g \beta}\right)^{1/2}$ [32], which for this silicon oil is $h_c = 2.5$ mm. For the LHC substrates, the liquid layer thickness was varied in the range of 550, 760 and 960 μ m. In case of the HHC substrates due to conductive heat losses across the substrate, the liquid layer thickness was decreased down to 100 μ m. After the layer was formed, the shutters of the heating and the probe lasers were opened. When the PTC signal reached a stationary state, its diameter, D_{st} , was measured with a ruler. Then both shutters were closed and the system was left for up to 10 min to cool down to room temperature and damping the thermocapillary flows in the layer. To control reproducibility the experiment was repeated five times for each substrate. Error of measurements did not exceeds 5%.

4 Experimental results and discussion

Figure 3 shows D_{st} of the PTC signal versus k_s in the logarithmic scale obtained for the LHC substrates for three thicknesses of the silicon oil layer at the power of the laser beam equals to 21 mW. For the HHC substrates, D_{st} versus k_s for the layer of 100 μ m thickness at the powers of the laser beam 21, 18 and 17 mW are shown in the logarithmic scale in Fig. 4. According to both Figs. 3 and 4, the dependency of D_{st} on k_s follows a power law $D_{st} \sim k_s^{-n}$, where the power exponent n increases from 0.672 ± 0.002

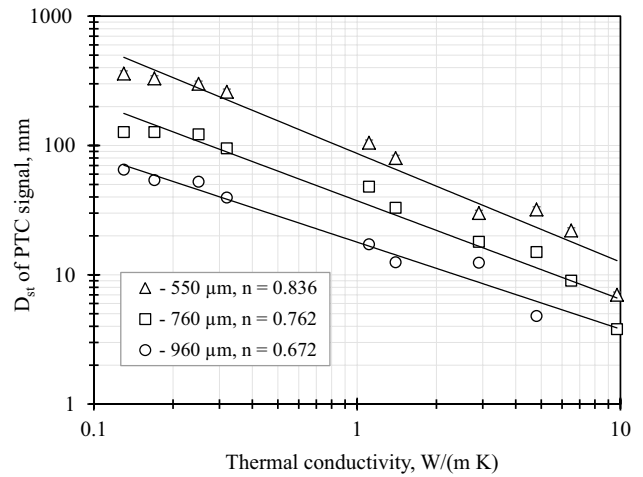


Fig. 3 The diameter of the PTC signal as a function of the thermal conductivity of substrates for different thicknesses of the liquid layer: 550, 760 and 960 μ m at the power of the heating beam 21 mW. The power exponents of fitting lines are shown in the legend

to 0.836 ± 0.003 when decreasing the layer thickness at constant P_h (Fig. 3) and lays in between 0.794 ± 0.001 and 0.899 ± 0.002 when changing the power of the heating laser beam at constant h_1 (Fig. 4). In the range of the high values of k_s the diameter of PTC signal for both types of the substrates reaches only a few millimeters. The PTC interference pattern has several bright and blurry rings that makes it difficult to be measured. This change in the pattern is related with substantial decreasing the depth of the thermocapillary dimple. When further increasing k_s the circular interference structure of the PTC signal transforms to a light spot with the gauss distribution of

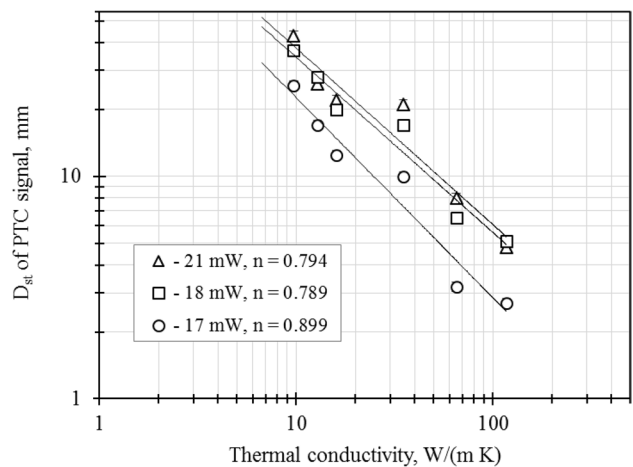


Fig. 4 The diameter of the PTC signal as a function of the thermal conductivity of the metallic substrates for thicknesses of the liquid layer 100 μ m at the powers of the heating beam 17, 18 and 21 mW. The power exponents of fitting lines are shown in the legend

the intensity, called as a zero-signal. This limit case corresponds to the reflection of the probe laser beam from a flat liquid layer that is the layer with zero curvature of the free surface. Thus, it is possible to conclude that there is a critical value of k_s^* at which the thermocapillary deformation of the free surface of the liquid layer becomes fully damped. The critical k_s^* in turn is related to the thickness of the liquid layer and the power of the heating laser beam. For instance, at $P_h = 21$ mW for the layers of 960 and 550 μm the zero-signal appears at $k_s^* = 6.5$ W/(m K) (the case is shown in Fig. 3 no experimental points obtained at $k_s \geq k_s^*$) and $k_s^* = 16$ W/(m K) (Rose's metal is not shown in Fig. 3), respectively. For the layer of $h_1 = 550$ μm at lowest power of the heating beam $P_h \cong 1$ mW the thermocapillary dimple decays starting from $k_s^* = 1.4$ W/(m K) (see Fig. 5). In the case of $h_1 = 100$ μm the zero-signal is detected on duralumin substrate with $k_s^* = 160$ W/(m K) at $P_h = 21$ mW.

It should be noted that there is another limit case, when the diameter of the PTC signal increases infinitely until disappearing, so no signal is observed on the screen in the end. This corresponds to the thermocapillary rupture of the liquid layer, when the solid substrate occurs to be free from a liquid in the irradiated area and, therefore, diffusely reflects the laser beam. In the current experiments, this situation was observed for $h_1 = 100$ μm at $P_h = 17, \dots, 21$ mW on substrates with $k_s = 0.13, \dots, 6.5$ W/(m K).

Obviously, the reason for both the damping of the thermocapillary convection in the liquid layer and the thermocapillary rupture of the layer is the domination of one of the heat transfer mechanisms: the conductive heat transfer into the solid substrate or the convective heat transfer into the liquid. An estimation of the Peclet number $Pe = vd\rho C_p/k_l$ for silicon oil with a typical velocity

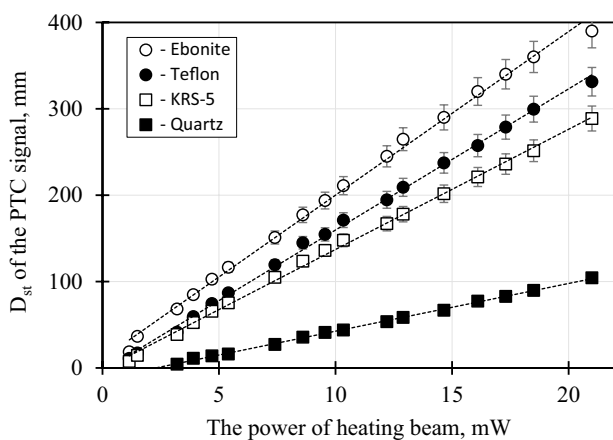


Fig. 5 The dependency of the diameter of the PTC signal on the power of the heating laser beam for substrates with different thermal conductivities: ebonite—0.13 W/(m K), Teflon—0.25 W/(m K), KRS-5—0.32 W/(m K) and quartz glass—1.4 W/(m K)

of the thermocapillary flow $v \sim 1$ cm/s and the width of the heated area equal to the beam diameter $d = 2.5$ mm, gives the value $Pe \approx 300$. The latter means that the heat flow into the liquid layer is caused by the convective heat exchange, whereas the heat flow into the solid substrates occurs due to the conductive heat transfer. In the range of substantial changing of D_{st} for both types of substrates, the convective heat transfer dominates over the conductive one and the thermocapillary convection in the layer is pronounced. When the thermal conductivity of substrate becomes high enough the conductive heat transfer starts to dominate decreasing the temperature of the heated area. As a result, temperature of the free surface of the liquid layer decreases; hence, the radial gradient of temperature along the free surface (see Eq. 4) becomes insufficient to generate the thermocapillary stresses required for the layer deformation.

Note that the power of the heating laser beam influences the sensitivity of the laser-induced thermocapillary effect to the thermal conductivity of substrates. In Fig. 5 the D_{st} as a function of P_h for the LHC substrates (such as ebonite, Teflon, KRS-5 and quartz glass) is presented for $h_1 \cong 550$ μm . As is seen in Fig. 5 the D_{st} linearly increases with the power of laser beam, $D_{st} \sim P_h$ for all substrates used. It is interesting to note that according to results [10, 33] the depth of the thermocapillary dimple also linearly increases with the power of the laser beam (a water layer) [10] and with temperature of an electrical heater embedded in a substrate (silicon oil on ebonite) [33]. As it follows from Fig. 5 the slope of the dependency D_{st} on P_h decreases with the increase in the thermal conductivity of substrate. This suggests that the dissipation of power into a substrate increases that leads to lowering the temperature gradient at the free liquid surface required for development of the thermocapillary dimple.

As mentioned above, the PTC signal is influenced by hydrodynamical factor as well. In Fig. 3 it is clearly seen that D_{st} for a given substrate decreases with the increasing of h_1 . Those results are quite expectative and are in accordance with the previous results [6]. Obviously when increasing the thickness of the layer, a resistance to the reverse bottom flow, which can be considered as flow with a parabolic velocity profile in a slit-like channel of $2h_1/3$ thickness, decreases. Therefore, the depth of the thermocapillary dimple becomes smaller and, consequently, the smaller D_{st} of the PTC signal. The sensitivity of the thermocapillary effect to h_1 (determined as ratio $\Delta D_{st}/\Delta h_1$, where $\Delta h_1 = 410$ μm) as a function of k_s for the LHC substrates at the constant P_h is presented in Fig. 6. The values of $\Delta D_{st}/\Delta h_1$ are negative because an increase in h_1 causes a decrease in D_{st} . The absolute value of $\Delta D_{st}/\Delta h_1$ decreases non-monotonically with the increasing k_s . In the range of $k_s^* > 3$ W/(m K) the increment of the thickness has a negligible effect on D_{st} . That is the influence of the thermal conductivity of substrates on

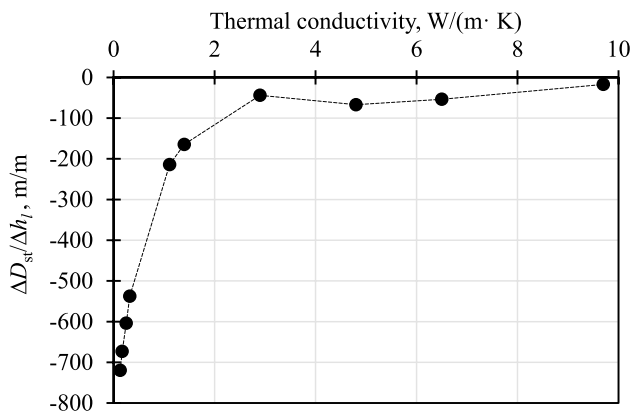


Fig. 6 The sensitivity of the thermocapillary effect to the variation of the thickness of the layer as a function of the thermal conductivity of substrates at constant $P_h = 21$ mW. The increment of the thickness of the liquid layer equals to $\Delta h_l = 410$ μm

the thermocapillary effect becomes prevalent in comparison with that of the layer thickness.

Interestingly that revealed in our experiments the reverse dependency $D_{st} \sim 1/k_s^n$ correlates with those determined in a number of photothermal methods [34–36]. We suggest that the sensitivity of the PTC signal to the thermal conductivity of substrates may be used as a basis for a new photothermocapillary method for the thermal conductivity measurements of solid samples.

5 Conclusions

The influence of the thermal conductivity of solid substrates on the thermocapillary effect induced by the laser beam in a thin liquid layer deposited on those substrates was studied experimentally. For quantitative analysis, the diameter PTC signal—the circular interference pattern formed on a screen by the probe laser beam reflected from the free surface of the liquid layer deformed by the thermocapillary flows was plotted as a function of the thermal conductivity. It was revealed that D_{st} of the PTC signal varies with k_s as $1/k_s^n$ in a wide range of k_s values, where n is the rate of the changing D_{st} , which depends on the thickness of liquid layer and the power of the heating beam. Increasing the k_s of substrates leads the decreasing thermocapillary deformation of the layer, and consequently the decreasing D_{st} , due rising the conductive losses of heat in substrate material. At some critical value of the thermal conductivity of substrate, the latter works as a heat sink lowering the thermal disturbance on the free liquid surface; as a result the thermocapillary deformation of the liquid layer becomes fully damped. A variation of D_{st} for a given substrate with the power of the laser beam is similar to the variation of the depth of the thermocapillary dimple with temperature of the heater embedded flush with the substrate

[33]. The sensitivity to the thickness of the liquid layer decreases non-monotonically with the k_s increasing at the constant power of the heating beam. The findings obtained above clearly demonstrate that thermal conductivity of substrate is very crucial parameter affecting the laser-induced thermocapillary effect and has to be taken into account when planning the experiments or developing methods for laser diagnostics of material properties.

Acknowledgements The research was supported by the RFBR (Grant No. 17-08-00291) and the Ministry of Education and Science of the Russian Federation (Grant No. 1019).

References

1. Y. Bayazitoglu, T.T. Lam, Marangoni convection in irradiating fluids. *J. Heat Transf.* **109**, 717–721 (1987)
2. A. Oron, Nonlinear dynamics of irradiated thin volatile liquid films. *Phys. Fluids* **12**, 29–41 (2000)
3. J.P. Longtin, K. Hijikata, K. Ogawa, Laser-induced surface-tension-driven flows in liquids. *Int. J. Heat Mass Transf.* **42**, 85–93 (1999)
4. S.P. Karlov, D.A. Kazenin, B.I. Myznikova, I.I. Wertgeim, Experimental and numerical study of the Marangoni convection due to localized laser heating. *J. Non-Equilib. Thermodyn.* **30**, 283–304 (2005)
5. H.M.J.M. Wedershoven, C.W.J. Berendsen, J.C.H. Zeegers, A.A. Darhuber, Infrared-laser-induced thermocapillary deformation and destabilization of thin liquid films on moving substrates. *Phys. Rev. Appl.* **3**, 024005 (2015)
6. B.A. Bezuglyi, O.A. Tarasov, Optical properties of a thermocapillary depression. *Opt. Spectr.* **92**, 609–613 (2002)
7. G. Da Costa, J. Calatroni, Self-holograms of laser-induced surface depressions in heavy hydrocarbons. *Appl. Opt.* **17**, 2381–2385 (1978)
8. G. Da Costa, J. Calatroni, Transient deformation of liquid surfaces by laser-induced thermocapillarity. *Appl. Opt.* **18**, 233–235 (1979)
9. G. Da Costa, R. Escalona, Time evolution of the caustics of a laser heated liquid film. *Appl. Opt.* **29**, 1023–1033 (1990)
10. H. Helmers, W. Witte, Holographic study of laser-induced liquid surface deformations. *Opt. Commun.* **49**, 21–23 (1984)
11. B.A. Bezuglyi, A.A. Fedorets, Measuring the thickness of thin liquid films on solid surfaces using the laser-induced thermocapillary response. *Tech. Phys. Lett.* **27**, 359–361 (2001)
12. B.A. Bezuglyi, O.A. Tarasov, Sensitivity of the thermocapillary method of thickness determination for transparent liquid films on horizontal absorbing substrates. *Tech. Phys. Lett.* **30**, 138–140 (2004)
13. B.A. Bezuglyi, O.A. Tarasov, S.I. Chemodanov, Method of contactless measuring of liquid viscosity. Patent RF 2305271, BI 24, (2007)
14. B.A. Bezuglyi, O.A. Tarasov, A.A. Fedorets, Modified tilting-plate method for measuring contact angles. *Coll. J.* **63**, 668–674 (2001)
15. B.A. Bezuglyi, S.I. Chemodanov, Effect of delay of the thermocapillary response of a transparent liquid layer during laser heating of the absorbing substrate. *Tech. Phys.* **50**, 1243–1245 (2005)
16. B.A. Bezuglyi, S.I. Chemodanov, O.A. Tarasov, New approach to diagnostics of organic impurities in water. *Colloid Surf. A* **239**, 11–17 (2004)

17. O.A. Tarasov, Evaluation of the possibility of using the laser-induced thermocapillary effect for photothermal spectroscopy. *Opt. Spectrosc.* **99**, 968–974 (2005)
18. B.A. Bezuglyi, AYu. Zykov, S.V. Semenov, Photothermocapillary diagnostics of near-surface flaws in a solid under a varnish-and-paint coating. *Russ. J. Nondestruct. Testing* **44**, 391–394 (2008)
19. B.A. Bezuglyi, AYu. Zykov, S.V. Semenov, Photothermocapillary method for detecting foreign inclusions in solids under paint and varnish coatings. *Tech. Phys. Lett.* **34**, 743–746 (2008)
20. B.A. Bezuglyi, AYu. Zykov, Photothermocapillary method for detecting delamination of paint and varnish Coatings. *Tech. Phys. Lett.* **35**, 650–652 (2009)
21. F. Du, J.R. Felts, X. Xie, J. Song, Y. Li, M.R. Rosenberger, A.E. Islam, S.H. Jin, S.N. Dunham, C. Zhang, W.L. Wilson, Y. Huang, W.P. King, J.A. Rogers, Laser-induced nanoscale thermocapillary flow for purification of aligned arrays of single-walled carbon nanotubes. *ACS Nano* **8**, 12641–12649 (2014)
22. N. Ivanova, V.M. Starov, A. Trybala, V.M. Flyagin, Removal of micrometer size particles from surfaces using laser-induced thermocapillary flow: experimental results. *J. Coll Interface Sci.* **473**, 120–125 (2016)
23. A. Oron, S.H. Davis, S.G. Bankoff, Long-scale evolution of thin liquid films. *Rev. Mod. Phys.* **69**(3), 931–980 (1997)
24. W.D. Ristenpart, P.G. Kim, C. Domingues, J. Wan, H.A. Stone, Influence of substrate conductivity on circulation reversal in evaporating drops. *Phys. Rev. Lett.* **99**, 234502 (2007)
25. D. Lide (ed.), *CRC Handbook of Chemistry and Physics*, 88th edn. (CRC Press, Boca Raton, 2007)
26. W.J. Tropf, M.E. Thomas, T.J. Harris, Properties of crystals and glasses, in *Handbook of optics*, vol. 2, Chp. 33, ed. by M. Bass, E.W. van Stryland, D.R. Williams, W.L. Wolfe (McGraw-Hill, New York, 1995)
27. Thermophysical properties of materials for nuclear engineering, *a tutorial and collection of data* (International Atomic Energy Agency, Vienna, 2008)
28. P. Amaral, A. Correia, L. Lopes, P. Rebola, A. Pinho, J.C. Lopes, On the use of thermal properties for characterizing dimension stones. *Key Eng. Mater.* **548**, 231–238 (2013)
29. J.H. Lienhard, J.H. Lienhard, *A heat transfer textbook*, 3rd edn. (Phlogiston Press Cambridge, Massachusetts, 2005)
30. J.E. Mark (ed.), *Polymer data handbook* (Oxford University Press, New York, 1999)
31. A. Juel, J.M. Burgess, W.D. McCormick, J.B. Swift, H.L. Swinney, Surface tension-driven convection patterns in two liquid layers. *Physica D* **143**, 169–186 (2000)
32. E.D. Éidelman, Influence of the thickness of the liquid layer on the ratio of the dimensions of a convection cell. *Tech. Phys.* **43**, 1275–1279 (1998)
33. B.A. Bezuglyi, V.M. Flyagin, Thermocapillary convection in a liquid layer with a quasi-point heat source in the substrate. *Fluid Dyn.* **42**, 978–986 (2007)
34. D. Dădărlat, M. Chirtoc, C. Nemațu, R.M. Căndea, D. Bicanic, Inverse photopyroelectric detection method. *Phys. Status Solidi A* **121**, 231–234 (1990)
35. J.A. Sell, D.M. Heffelfinger, P. Ventzek, R.M. Gilgenbach, Laser beam deflection as a probe of laser ablation of materials. *Appl. Phys. Lett.* **55**, 2435–2437 (1989)
36. J.P. Gordon, R.C.C. Leite, R.S. Moore, S.P.S. Porto, J.R. Whinnery, *Bull. Am. Phys. Soc.* **9**, 501 (1964)